Plasma Sci. Technol. **20** (2018) 065504 (10pp) https://doi.org/10.1088/2058-6272/aaaadd

Influence of dielectric barrier discharge treatment on mechanical and dyeing properties of wool

Rahul NAVIK[1,2], Sameera SHAFI[2], Md Miskatul ALAM[1], Md Amjad FAROOQ[2], Lina LIN (林丽娜)[1,3] and Yingjie CAI (蔡映杰)[1,3]

[1] Hubei Provincial Engineering Laboratory for Clean Production and High Value Utilization of Bio-Based Textile Materials, Wuhan Textile University, Wuhan 430073, People's Republic of China
[2] School of Chemistry and Chemical Engineering, Shanghai Jiao Tong University, Shanghai 200240, People's Republic of China

E-mail: linalin@wtu.edu.cn and yingjiecai@wtu.edu.cn

Received 7 December 2017, revised 26 January 2018
Accepted for publication 26 January 2018
Published 30 April 2018

Abstract

Physical and chemical properties of wool surface significantly affect the absorbency, rate of dye bath exhaustion and fixation of the industrial dyes. Hence, surface modification is a necessary operation prior to coloration process in wool wet processing industries. Plasma treatment is an effective alternative for physiochemical modification of wool surface. However, optimum processing parameters to get the expected modification are still under investigation, hence this technology is still under development in the wool wet processing industries. Therefore, in this paper, treatment parameters with the help of simple dielectric barrier discharge plasma reactor and air as a plasma gas, which could be a promising combination for treatment of wool substrate at industrial scale were schematically studied, and their influence on the water absorbency, mechanical, and dyeing properties of twill woven wool fabric samples are reported. It is expected that the results will assist to the wool coloration industries to improve the dyeing processes.

Keywords: air plasma, reactive dye, surface energy, wool

(Some figures may appear in colour only in the online journal)

1. Introduction

Wool is mostly used in winter conditions for the desired level of comfort to a wearer. The core and shell structure, crimp and hydrophilic nature, and light weight of the fiber make it a promising material for winter clothing [1–4]. Generally, the fiber undergoes different wet treatment processes prior to the garment manufacturing to obtain the desired level of aesthetic appearance and feel. The outer layers of the fiber are highly hydrophobic, therefore it acts as a barrier for penetration of the chemicals and colorants during wet processing [5–7]. Hence various chemical processes have been proposed and implemented over time at a commercial scale to modify the fiber from hydrophobic to hydrophilic. However, the chemical methods to modify the fibers properties lead to the environment pollution and consume a huge amount of energy, water, and chemicals [8]. Finally, it includes an additional cost to the final product and treatment of effluent before discharge.

In general, the conventional dyeing technologies have low color yield, lack of shade uniformity and unpleasant aesthetic appearance to the final product [9, 10]. In this context, the surface characteristics directly influences the hygroscopic behavior of the fibrous materials [11, 12]. Therefore, extensive efforts have been given to modify the surface of the wool for rapid penetration of chemicals and colorants (natural and synthetic) during dyeing and finishing operations [7, 13–15]. Plasma technology is an alternative and cost effective proven method for surface modification of natural and synthetic fibers [16–20]. The treatment of wool

[3] Authors to whom any correspondence should be addressed.

with plasma technology can promote the diffusion of organic molecules inside the fibers to enhance the dyeing rate, color fastness, wash resistance, and strong adhesion of coating with fibers. Furthermore, the high diffusion rate of organic molecules inside the fibers decreases the amount of chemicals, and colorants to achieve the desired appearance and functionalities [4, 10, 21–23]. The improved properties as a plasma treatment is mainly originated from chemical as well as physical modification. However, the resultant nature of the wool substrate depends upon the nature of the plasma medium used [3, 9].

The atmospheric pressure cold plasma technologies are widely used for processing of textiles because most of the textile fibers are heat sensitive. Among other plasma reactors, one of the most exciting technologies emerged in recent years is that dielectric barrier discharge (DBD) plasma reactor operating in the atmospheric air [24–26]. This plasma reactor possesses many advantages such as continuous processing, large surface area, and short treatment duration to get the desired effects up to 1000 Å scale depth without any adverse effects on the bulk properties of the materials [18, 25]. However, there is currently little published work of plasma processing of wool fibers by DBD and specific effects of varying operating parameters on the resulting surface treatment outcomes. Hence, this study reports the effect of DBD treatment duration on the hygroscopic, mechanical, and dyeing properties of twill woven wool fabric samples.

2. Experimental

2.1. Materials

The wool fabric (100%) has a warp density of 50 threads cm^{-1}, weft density of 45 threads cm^{-1}, and the average mass of 75 g m^{-2}. Reactive Red 195 dye was purchased from the Shanghai Jiaying Chemical Co. Ltd (China) and it was used as received without any purification. Non-ionic detergent based on alkylaryl polyglycol ether was purchased from the Sinopharm chemical reagent. Other reagents used were laboratory grade.

2.2. Plasma treatment

Before plasma treatment, the wool fabric was washed with non-ionic detergent (2 g l^{-1}) at 60 °C for 2 h and dried at ambient temperature. The surface treatment of specimens was carried out using atmospheric pressure air plasma in a DBD reactor as described elsewhere [15]. A line diagram of the plasma reactor used in this study is shown in figure 1. The reactor has a pair of Al_2O_3 ceramic electrodes with an effective area of 400 mm × 500 mm. The specimens were taped on the bottom electrode and a gap of 2 mm was maintained from top electrodes during treatment. A high frequency, 44.0 kHz power supply was used to generate plasma and the specimens were treated for 150 s, 300 s, and 450 s respectively. After plasma treatment, the wool fabric was conditioned at 27 °C ± 2 °C and 65% relative humidity prior to further use.

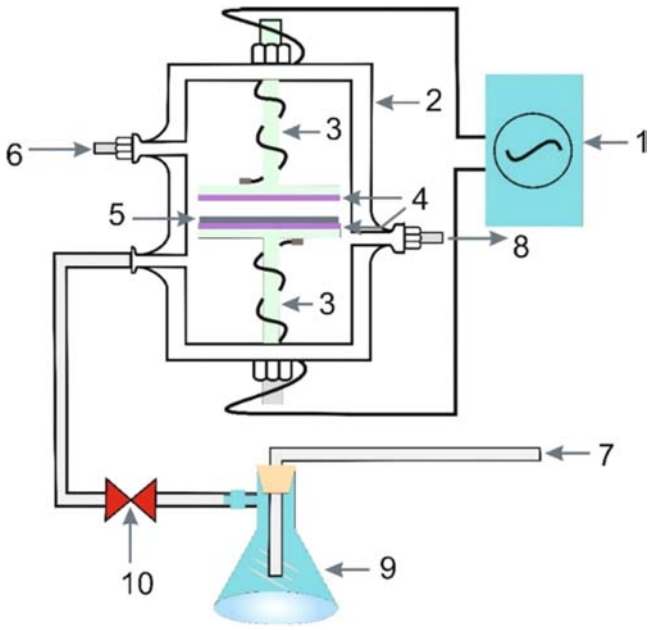

Figure 1. Experimental DBD plasma reactor operating at atmospheric pressure; 1—high voltage power supply, 2—reactor body, 3—Al_2O_3 ceramic electrode, 4—barrier film (polyimide), 5—wool substrate, 6 and 7—gas inlet, 8—gas outlet, 9—solvent box (ethanol or acetone), 10—gas flow control valve.

2.3. Characterizations

The Fourier Transform infrared (FTIR) spectra of the specimens were recorded with a Nicolet Avatar 360 FTIR spectrophotometer (Madison, USA). The x-ray Photoelectron Spectroscopy (XPS) data was collected on VG Scientific ESCALAB 200A instrument, which was supplied with an Al Kα x-ray source of 1486.6 eV in a vacuum (~10^{-7} Pa). The Atomic Force Microscope (AFM) measurements were performed on a scanning probe microscope (NanoNavi/E-Sweep, SII NanoTechnology, Inc. Japan) with environmental control. The wool substrates were measured with the vibrating mode to measure the force distance on the cantilever as the AFM tip experiences changed in the adhesion. The AFM data was obtained with the NanoScope Analysis 1.8 version software. Also, the surface topology of the untreated and the treated fibers was analyzed with an ultra-high resolution Field Emission Gun Scanning Electron Microscope (NOVA 200 Nano SEM, FEI Company, USA). The temperature within the DBD equipment with and without the wool substrates was measured with an Omega Teflon coated thermocouple. A V/°C analog-to-digital converter was used to regulate the thermo-couple. LABVIEW software was used to gather the thermal data. The wicking height of the untreated and the treated specimens was recorded using the DIN 53 924 test method. The contact angle and the calculation of surface free energy [2] of the specimens was measured with an Easy Drop Analyzer instrument (Zhongchen Digital Technique Apparatus Co. Ltd, China). Each sample was analyzed 20 times and the average value of the water contact angles was used to calculate the work of adhesion (W_{Adh}) according to

Table 1. Surface energy components of the liquid used for analysis.

Surface energy	Distilled water	PEG 200	Glycerol
γ (mJ m^{-2})	72.80	43.50	63.40
γ^{D} (mJ m^{-2})	29.10	29.90	37.40
γ^{P} (mJ m^{-2})	43.70	13.60	26.00

the Young–Dupré equation (equation (1)).

$$W_{\mathrm{Adh}} = \gamma_1 \times (1 + \cos\theta), \tag{1}$$

where, γ_1 is the surface tension of water and θ is the contact angle in degrees. In the case of polar solids or liquids, the total γ is a combination of the London dispersion forces (γ^{D}) and the polar forces (γ^{P}) of the material (equation (2)). The polar component (γ^{P}) and the dispersive component (γ^{D}) of the surface energy were calculated according to the Wu method, using equation (3). The liquids of known surface energy were utilized for the surface energy measurement (table 1).

$$\gamma = \gamma^{D} + \gamma^{P} \tag{2}$$

$$\gamma_{sl} = \gamma_s + \gamma_1 - 4\left(\frac{\gamma_s^{D}\gamma_1^{D}}{\gamma_s^{D} + \gamma_1^{D}} + \frac{\gamma_s^{P}\gamma_1^{P}}{\gamma_s^{P} + \gamma_1^{P}}\right), \tag{3}$$

where, γ_{s1} is the interfacial tension between liquid and solid, γ_s is the surface tension of solid, γ_s^{D} and γ_s^{P} are the London dispersion forces and the polar forces of the solid, γ_1^{D} and γ_1^{P} are the London dispersion forces and the polar forces of the liquid.

The breaking strength of the specimen was measured according to the ASTM D5034-9 test method using the 'INSTRON 4202 tensile strength tester (James Heal, UK). The tear strength was measured with the ASTM D2261-13 test method using the Elma-tear tear strength tester (James Heal, UK).

2.4. Dyeing method

In a typical dyeing procedure, the untreated and treated wool specimens (1 g each) were dyed at room temperature for 15 min in 0.5%, 1.0%, 3.0%, 5.0%, and 7% on mass of fiber (omf) shades at a fabric to liquor ratio of 1:25 in a rotary infrared dyeing machine (Mathis, Brazil). Then the temperature of the dyebath was raised to 50 °C and Albegal FFA (0.5 mg ml^{-1}) and Albegal B (1 mg ml^{-1}) were added to the bath. The pH of the dye bath was maintained in the range 5.0–6.0 with the help of 2% owf acetic acid (80%). Subsequently the temperature of the dyebath was raised to 100 °C and the wool specimens were treated for additional 60 min. After dyeing the dyed specimens were washed off in a 50% of urea solution at a liquor ratio of 1:100. The washed specimens were air dried at an ambient temperature for characterization.

2.5. Dye bath exhaustion measurement

The resultant dye liquors were diluted to a constant volume using deionized water. Their corresponding absorbance was recorded with an Ultraviolet–Visible spectrophotometer (Hitachi U-400, Japan) at a maximum absorbance wavelength. The exhaustion ($\%E$) was calculated with equation (4).

$$\%E = \frac{A_0 - A_1}{A_0} \times 100, \tag{4}$$

where A_0 and A_1 are the absorbance values of the dye bath before and after dyeing.

2.6. Dye fixation measurement

The K/S values of the dyed specimens were calculated using a Datacolor 110 spectrophotometer (Datacolor 110, USA) in order to calculate the percent fixation ($\%F$) of the dye on the specimens with equation (5). Each specimen was scanned at 20 random places.

$$\%F = \frac{(K/S)_2}{(K/S)_1} \times 100, \tag{5}$$

where $(K/S)_1$ and $(K/S)_2$ are the Kubelka Munk values of the dyed samples before and after soaping.

2.7. Color strength and color uniformity measurements

The standard deviation of above measured K/S values was expressed as $\sigma_{(\lambda)}$ and was calculated using equations (6) and (7).

$$\overline{(K/S)_\lambda} = \frac{1}{n}\sum_{i=1}^{n}(K/S)_{i,\lambda} \tag{6}$$

$$\sigma_\lambda = \sqrt{\frac{\sum_{i=1}^{n}[(K/S)_{i,\lambda} - \overline{(K/S)_\lambda}]^2}{n-1}}, \tag{7}$$

where, $\overline{(K/S)_\lambda}$ is the average value of $(K/S)_{i,\lambda}$, $(K/S)_{i,\lambda}$ is the K/S value of each random spot, λ is the maximum absorption wavelength, n is the number of measurement at different places of the sample, and σ_λ is the standard deviation of each random area's K/S value with $(K/S)_\lambda$.

2.8. Color fastness properties

The washing and the rubbing fastness properties of the specimens were measured according to the ISO 105-CO6 (C2S test number) and ISO 105X 12:2001 test methods. The light fastness was determined in an accelerated weathering tester equipped with an UVA 340 lamp. The samples were exposed for 12 and 24 h. The extent of color degradation was examined on an ISO gray scale.

3. Results and discussion

3.1. Surface chemical composition analysis

The XPS is a powerful tool used to measure the chemical composition of materials. As shown in table 2, the atomic ratio of O/C increased from 0.17 to 0.25 in regard to the plasma treatment time. The increased oxygen content was likely due to the oxidation of the hydrocarbon chains in the wool substrates. The amount of N atom was not altered considerably. However, a

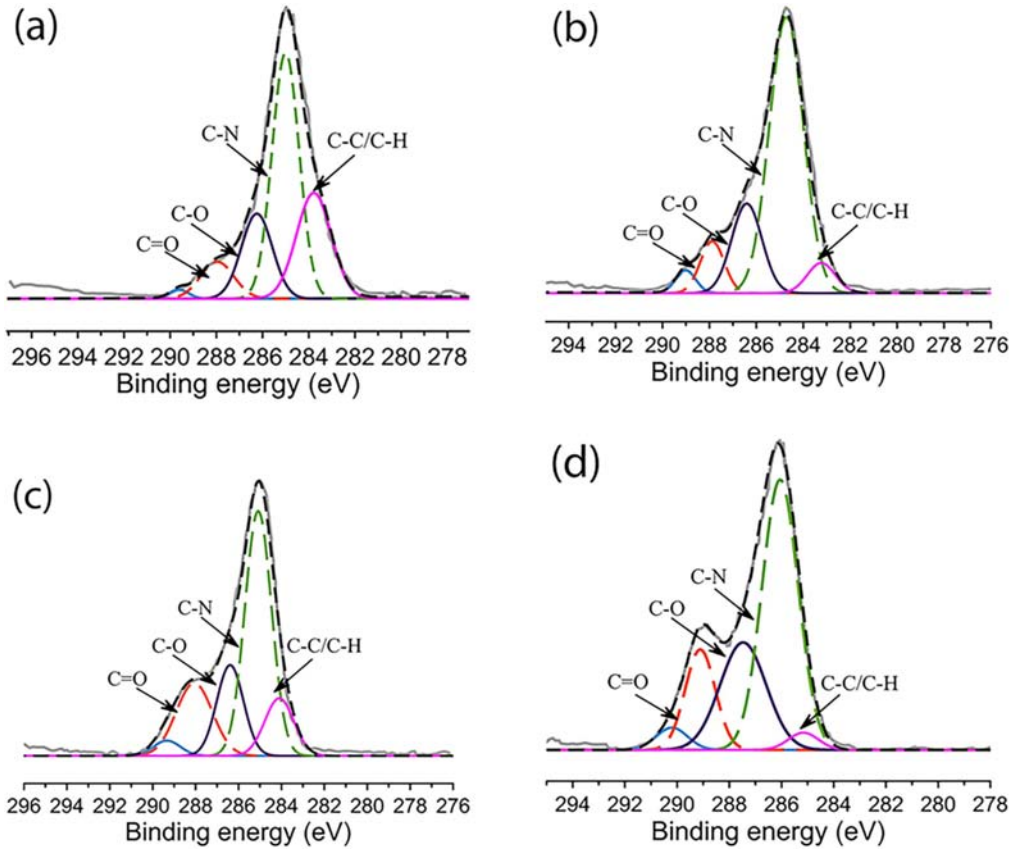

Figure 2. XPS C1S core level spectra of (a) the untreated and (b) the plasma treated wool substrate for 150 s, (c) 300 s, and (d) 450 s.

Table 2. Elemental compositions and atomic ratios of the untreated and the plasma treated wool substrates.

	Atomic composition (%)				Atomic ratios			Relative chemical bond area C1S (%)			
Treatment time (s)	C	O	N	S	O/C	N/C	S/C	C–C/C–H (283.8 eV)	C–N/C–S (285.6 eV)	C=O (286.4 eV)	O–C=O (288.3 eV)
Untreated	78.53	13.87	5.46	2.14	0.17	0.06	0.02	57.41	20.65	14.46	7.48
150	76.38	16.28	5.24	2.10	0.28	0.06	0.02	54.21	21.07	15.38	9.34
300	75.55	17.87	4.56	2.02	0.23	0.06	0.02	51.53	22.17	16.09	10.21
450	74.56	19.33	4.13	1.98	0.25	0.05	0.02	49.41	22.05	17.39	11.15

slight reduction in the sulfur atoms was also observed due to the etching of the of the sulfur rich cuticle layer.

As shown in figure 2, the peak deconvolution of the obtained spectrum exerted the characteristic peaks of C–C/C–H, C–N/C–S, C–O, and C=O carbon containing groups at 283.8 eV, 285.6 eV, 286.4 eV, and 283 eV respectively. The peak area of the C–N/C–S, C–O, and C=O were significantly increased, which strongly supported that the plasma treatment increased the oxygen containing functionalities such as hydroxyl and carboxyl groups. However, the results were different with different treatment durations. The sample treated for 450 s obtained a higher reduction of the C–C/C–H group than the samples treated for 150 and 300 s due to lower oxidation degree in limited duration.

The FTIR measurements also performed to analyze the change in the chemical groups of wool substrates after plasma treatment. As shown in figure 3, the FTIR spectrum of the untreated specimen showed intense peak of –OH stretching vibration at 3292 cm^{-1}. There were symmetrical and asymmetrical stretching bands of CH_2 and CH_3 at 2800–3000 cm^{-1} [19, 27]. The transmittance bands at 1635 and 1519 cm^{-1} corresponded to the amide I band of the amide carbonyl C=O stretching vibration and the amide II bands of the N–H bending motion [28, 29]. The peaks positioned at 1745, 1234, and 1041 cm^{-1} were the primary characteristic peaks of the thioester group, the Bunte salt, and the Cysteine-sulfonate of amide III. The plasma treated specimens obtained the intensities of $–CH_3$ and CH_2 peaks between the 2800 and 3000 cm^{-1} regions, which decreased and disappeared after the 450 s treatment due to oxidative splitting of the fatty layer [27] and formation of low molecular weight etched materials.

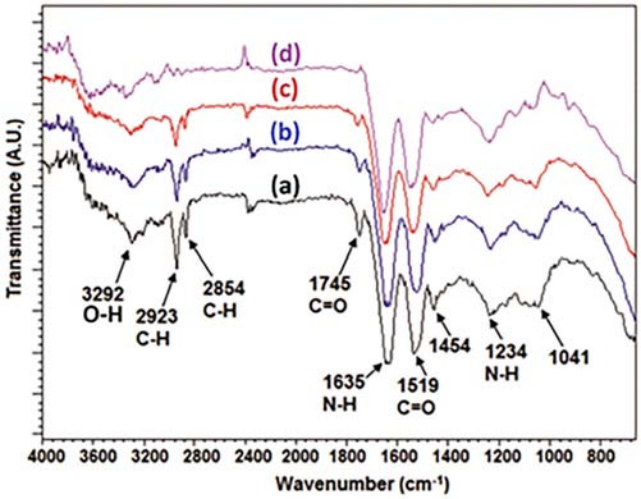

Figure 3. FTIR spectra of (a) the untreated and (b) the plasma treated wool fabrics, treated for 150 s, (c) 300 s, and (d) 450 s.

According to the previous report [30], the bombardment of the high energy radicals, which were generated in air plasma could break the bonds of less than 10 eV energy on the polymer chains. These broken chains in contact with the reactive species could generate low molecular weight molecules containing –COO and C=O groups. Thus, CH_2 and CH_3 groups were gradually reduced with respect to the treatment duration. There was a slight broadening and absorption observed in the 2993–3292 cm^{-1} regions, which corresponded to the –OH and the –NH groups. The region corresponded to the amide I and the amide III ranging from 1700 to 1200 cm^{-1}, where it exhibited identical behavior to the untreated specimen. The transmittance intensity of the cystic acid band at 1041 cm^{-1} decreased considerably, because of the increased cystic acid from the cleavages of the disulfide linkages. The results clearly demonstrated that the reactive species of the DBD plasma oxidized the main functional groups of the wool fiber into the hydrophilic groups. The changes in the functional groups led to the absorbency and reactivity of the fiber.

3.2. Surface topology analysis

The surface topology of the untreated and the treated substrates was studied with SEM measurements. As shown in figure 4, the surface appearance of the untreated wool fiber was stepped scale structure. Whereas, the surface topology of the treated fiber exerted a damage to the scales by the bombardment of the high energetic electrons. Some nano cracks and grooves on the surface were also formed [7, 13]. However, these nano size cracks and grooves were difficult to detect because of the complex scale structure of these wool fibers and limitation of the precision of the instrument. Therefore, the surface topology of the substrates was analyzed using AFM.

As shown in figure 5, the three-dimensional AFM image of the pristine fiber showed a smooth topography, whereas the treated fiber surface showed a rough appearance with few new aggregates and pores of several sizes. A careful measurement of surface roughness showed that the average roughness (68–346 nm) of the untreated wool fiber was significantly lower than the average roughness of the plasma treated wool fiber (70–521 nm). The temperature of the reactor increased in the presence of wool substrate (figure 6). The increased temperature could be attributed to the radical formation and the recombination of the ions in the substrate, which was favorable to the surface etching of the wool fiber on a nanoscale [31]. Also the energetic electrons led to the succession of keratin molecular chains, and promoted the surface etching. Thus, roughness of the surface increased.

3.3. Absorbency

The dynamic contact angle was measured to investigate the influence of the plasma treatment on the wetting properties of the wool specimens. Sometimes, the dynamic contact angle measurement of the hydrophobic materials with irregular surface reduced the accuracy of the large contact angle values. Therefore, the specimens were further analyzed via the wicking height measurement. As shown in figure 7(a), the plasma treatment decreased the contact angle from 103° to 96°, 81°, and 74° after the treatment for 150 s, 300 s, and 450 s respectively. Also, the capillary rise rate was quicker on the plasma treated wool stripe than the untreated wool stripe (figure 7(b)). The untreated wool specimen had a wicking height of 8 mm after immersion for 30 min. The wicking height increased to 50 mm, 57 mm, and 69 mm after the plasma treatment for 150 s, 300 s, and 450 s respectively. The difference in the contact angle and wicking height with respect to the plasma treatment was likely due to the differences in degree of chemical modification of the fiber surfaces. Also, the longer treatment durations possibly roughened the hydrophobic layers to a larger extent and generated the microcracks on the surface of the fibers [32, 33]. Hence, the specimen treated for 450 s obtained a better wetting performance than the specimens treated for 300 and 150 s.

3.4. Surface energy measurement

The total surface energy (γ), the dispersive component (γ^D), the polar component (γ^P) of water, the polyethylene glycol (PEG), and the glycerol contact angle values were studied (table 3). The treated substrates presented higher surface energy values than the untreated wool substrates. The dispersive component of the substrates decreased from 3.67 to 1.62 mJ m^{-2}. The polar component increased from 0.20 to 17.62 mJ m^{-2}. The results were consistent with the previously reported work [2], where DBD plasma treatment increased the specific surface energy from approximately 4 to 60 mJ m^{-2}. The improvement of the surface energy was attributed to the partial decomposition of the outer lipid layers after the air plasma treatment and the formation of the new polar groups [34]. The oxidation of surface components increased the amount of oxygen containing groups (–OOH, –OH, and –C=H as per the C–C, the C–O, the C=O, and the O–C=O oxidation order) on the wool surface. Thus oxygen containing groups provided the wool fiber surface with high energy for absorbing the moisture [35].

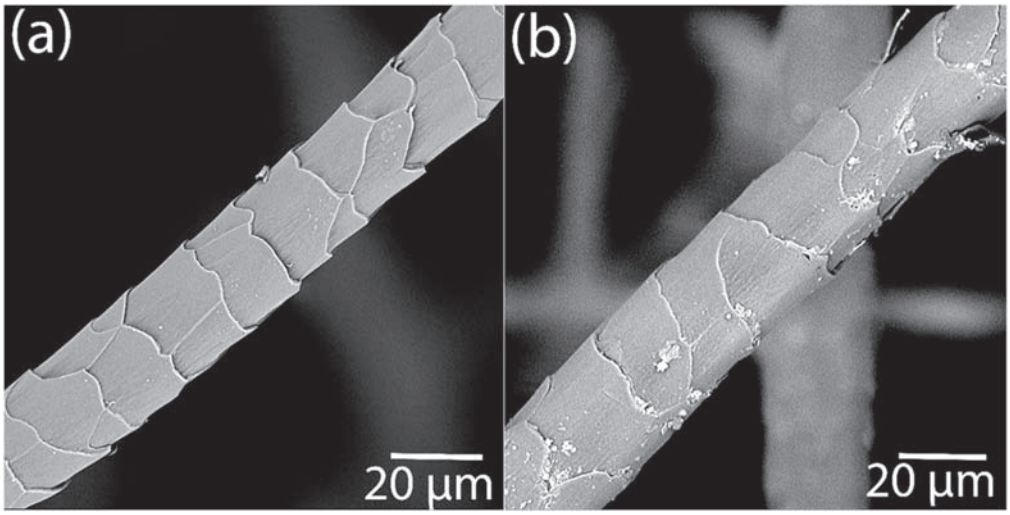

Figure 4. SEM images of (a) the untreated wool fiber and (b) the plasma treated wool for 450 s.

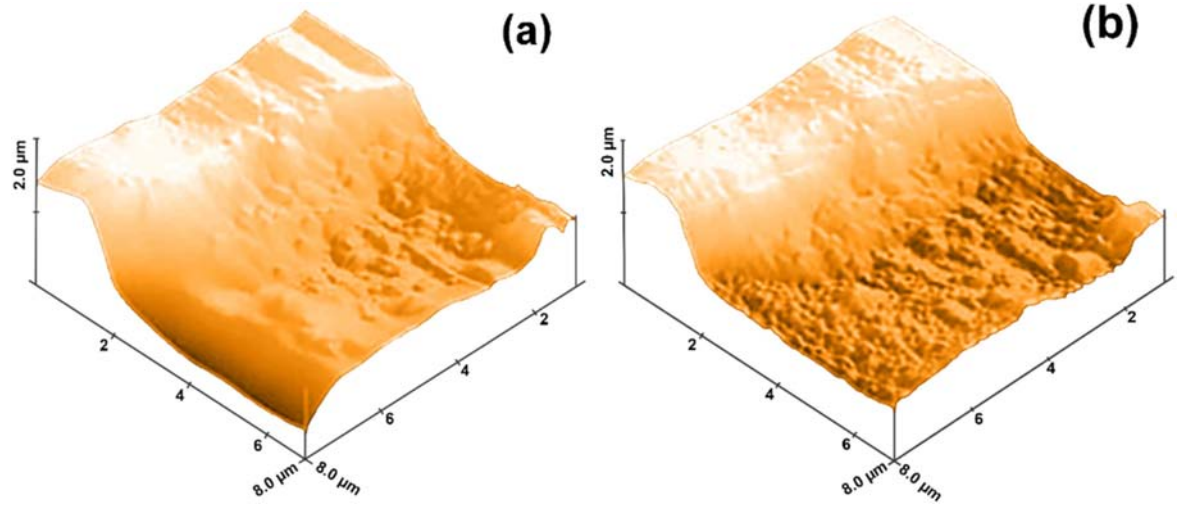

Figure 5. AFM images of (a) the untreated wool and (b) the plasma treated wool for 450 s ($10 \times 10\ \mu m^2$ scan areas).

3.5. Influence on dyeing characteristics

3.5.1. Exhaustion. As shown in figure 8(a), the exhaustion rate of the reactive dye improved significantly after the plasma treatment of the wool specimens. The exhaustion rate as a function of dyeing time was higher for the plasma treated wool specimen than the untreated specimen during the early stages of dyeing, as the dye omf increased from 0.5% to 3.0%. The increased exhaustion could be due to the increased affinity between the dye and the fiber after the plasma treatment. In addition, the high wetting ability and the presence of the nano-sized cracks on the treated wool specimens could have provided a pathway for the rapid diffusion of the dye molecules inside the fiber structure and improved the rate of the dye bath exhaustion. However, the longer treatment time, for 450 s, obtained a higher exhaustion value than the specimens treated for 150 and 300 s. The

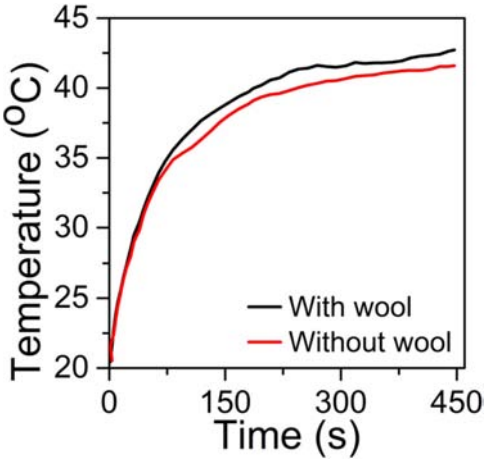

Figure 6. Temperature response inside the reactor with and without the wool substrate.

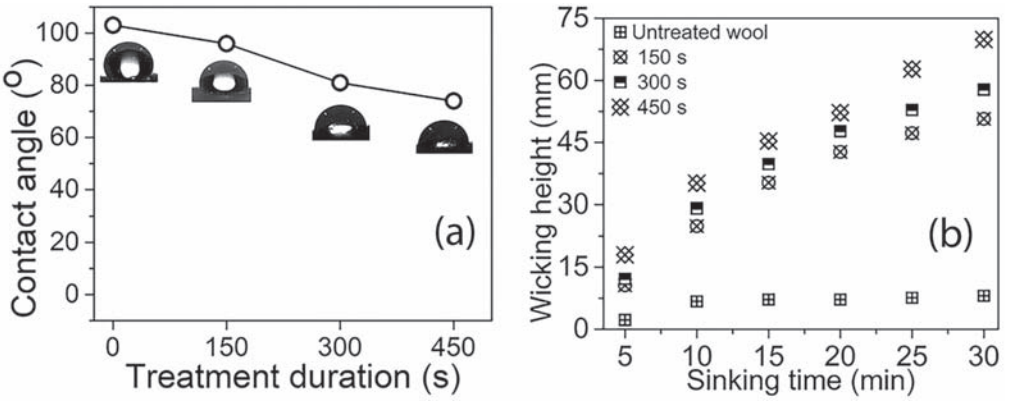

Figure 7. (a) Contact angles and (b) wicking heights as a function of sinking time on the untreated and the plasma treated wool fabrics.

Table 3. Average contact angle values, surface energy, and work of adhesion values of the untreated and the treated substrates.

Treatment duration (s)	θ_{water} (°)	θ_{PEG200} (°)	$\theta_{Glycerol}$ (°)	γ (mJ m^{-2})	γ^{D} (mJ m^{-2})	γ^{P} (mJ m^{-2})	W_{Adh} (mJ m^{-2})
0	153 ± 2.0	146.23 ± 2.2	148.92 ± 4.2	3.96	3.67	0.20	7.94
150	146 ± 1.8	93.31 ± 1.9	145.34 ± 6.2	8.72	4.42	0.45	12.43
300	131 ± 1.9	89.15 ± 2.3	134.53 ± 4.5	13.46	5.34	0.51	25.05
450	74 ± 3.5	61.82 ± 3.5	129.43 ± 1.6	18.38	1.62	17.62	92.94

difference in exhaustion is likely originated from the extent of chemical and physical modification when exposure to the plasma environment for different durations.

3.5.2. Fixation. The fixation of the reactive dyes is important for the production of light, medium, and dark shades, because a poor fixation property decreased the dye mass in the final dyed materials after washing. Figure 8(b) shows the $\%F$ values of the with and the without plasma treated wool specimens dyed. The $\%F$ values of the untreated wool fibers at various dye omf ranged from 70% to 78%. These values increased to 75%–80%, 76%–88%, and 78%–90% after the plasma treatment for 150, 300, and 450 s. The improvement of the $\%F$ value after the plasma treatment was attributed to the increased functional groups for better attachment of the dyes with fibers [36, 37]. Thus dyes were largely adsorbed on the plasma treated substrates via columbic forces. This subsequently promoted the covalent bonding between the adsorbed dyes and the reactive sites of the wool fibers. The chemically reacted dye molecules are difficult to be washed off. The low $\%F$ values in the case of untreated wool fibers suggested that after fixation, a number of dyes did not react with the wool fibers.

3.5.3. Color strength. As shown in figure 8(c), the K/S values were higher for the treated wool specimens than the untreated wool samples. The values increased as plasma treatment duration was increased. The difference in the K/S values were noticeable for the treated specimens, which were dyed with 7% dye omf. These specimens obtained higher color strength values than the untreated specimens. At a low dye omf, such as 0.5% and 1%, similar color strength values were achieved, because sufficient amounts of reactive sites for dye attachment with fibers were present.

3.5.4. Color uniformity. The standard deviation of the K/S values were used to calculate the color uniformity of the untreated and the treated specimens. As shown in figure 8(d), the treated wool specimens demonstrated a higher standard deviation value than the untreated wool specimens. Also the color uniformity decreased with the increased plasma treatment duration. In case of plasma treated samples, sample treated for 150 s exerted lower standard deviation value than the samples treated for 300 and 450 s respectively. This was caused by the slow rate of the dye adsorption from the bath. The increased functional groups for the dye caused rapid adsorption of the dye molecules on the fiber surfaces, thus samples treated for 300 and 450 s obtained higher standard deviation values. The color uniformity was also influenced by the dye omf due to the presence of excess amount of dye molecules in the bath for the fibers. The specimens dyed with 0.5%, 1%, and 3% omf obtained a lower standard deviation than the specimens dyed with 5% and 7% dye omf. This was likely due to the presence of excess amount of the dye molecules on the fiber surface, which was not completely removed during washing process, resulting a slight color difference, i.e. slightly higher standard deviation values.

3.6. Color fastness properties

The color fastness properties to washing, rubbing (dry and wet) and light of the untreated and plasma treated wool samples are presented in table 4. The extent of staining on the adjacent fibers was assessed visually, and then graded from 1 to 5 using an ISO gray scale (1—poor; 2—satisfactory; 3—moderate; 4—good; and 5—excellent). Despite

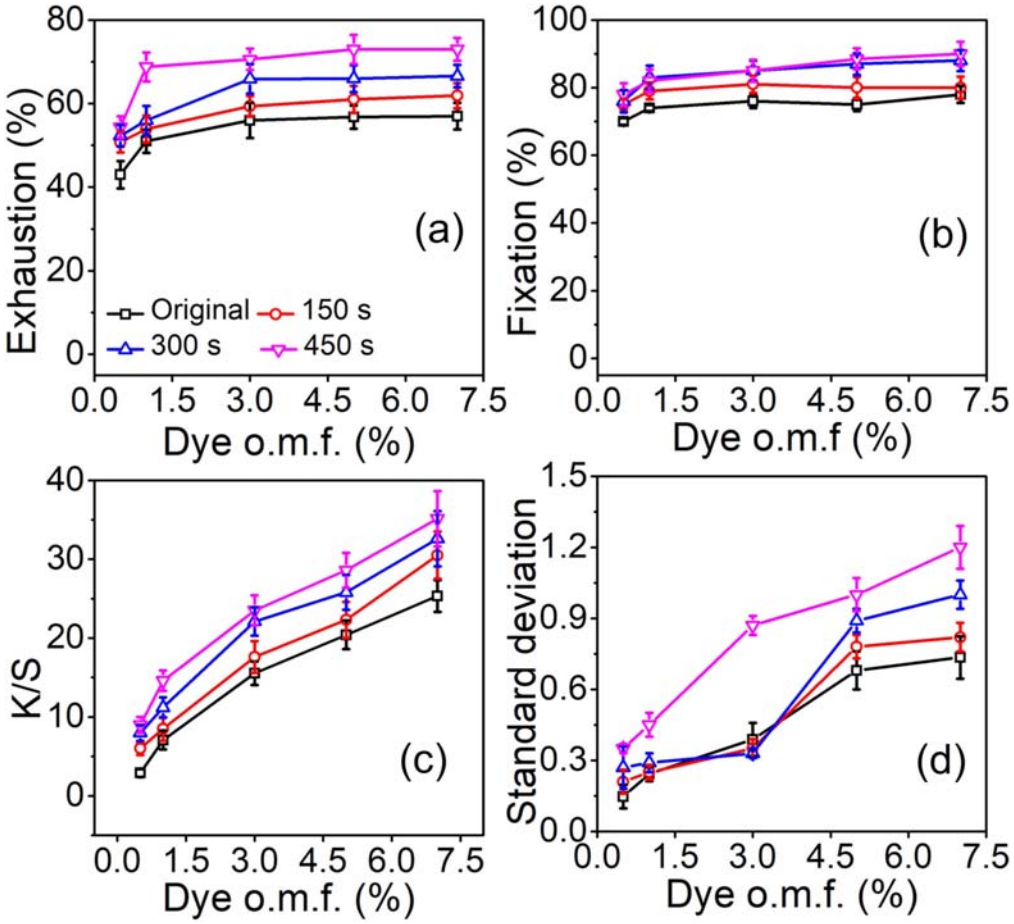

Figure 8. The influence of the plasma treatment on (a) the exhaustion, (b) the fixation, (c) the color strength, and (d) the color uniformity of reactive dye on wool fabric.

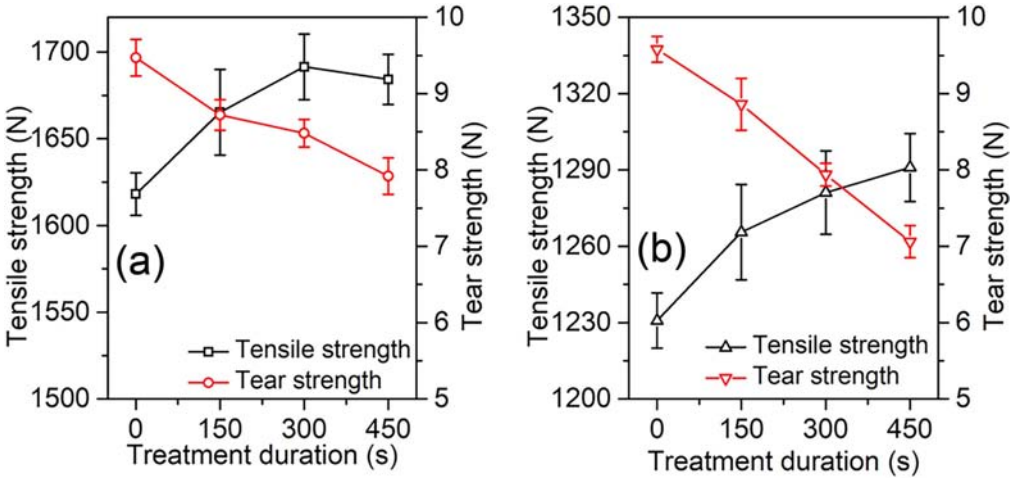

Figure 9. Tensile strength and tear strength of wool fabrics in (a) the warp direction, and (b) the weft direction.

the rapid dye diffusion, the results were good for the washing and rubbing fastness measurements. The dye deterioration was reduced during the light fastness measurements of the treated wool substrates. The value of 4–5 was obtained for all plasma treated specimens during the wash fastness measurement, due to a better fixation of the dye on the specimens. The dry rubbing fastness of the plasma treated samples obtained a grading of 3–4, even at higher dye omf shades. The wet rubbing fastness was slightly inferior for the specimens dyed with 5% and 7% dye omf, because of the excess amount of dye on the surface of these specimens. In the rubbing in wet condition, water acted as a lubricant for breaking the hydrogen bonds between the fiber and the dye molecules, which stained the

Table 4. Color fastness properties of wool fabric dyed with various omf of Reactive Red 195 for various plasma treatment durations.

	Dye omf (%)														
	Wash fastness (staining on cotton/on wool)					Rubbing fastness (dry/wet)					Light fastness (after 12 h/after 24 h)				
Duration (s)	0.5	1.0	3.0	5.0	7.0	0.5	1.0	3.0	5.0	7.0	0.5	1.0	3.0	5.0	7.0
Untreated	3–4/4	3–4/3–4	3–4/3–4	3/3–4	3/3–4	5/4	5/4	5/4	5/4	4/4	4/4	5/4–5	4–5/4	4/4	4/4
150	4–5/5	4–5/4–5	4–5/4–5	4/4–5	4/4–5	4–5/4–5	5/4–5	5/4–5	5/4	3/3	5/5	5/4–5	4–5/4	4/4	4/4
300	4–5/5	4–5/4–5	4–5/4–5	4/4–5	4/4–5	4–5/4–5	5/4–5	5/4–5	5/3	3/3	5/5	5/4	4–5/4	4/4	4/4
450	4–5/5	4–5/4–5	4–5/4–5	4/3–4	3/3–4	4–5/4–5	5/4–5	5/4–5	5/3	3/3	5/4	5/4	4–5/4	4/4	4/4

adjacent fabric. The light fastness of the specimens was evaluated after 12 and 24 h of exposure time. The treated samples presented a lower dye degradation, even after 24 h of exposure. A grading of 4–5 was obtained for the untreated and the plasma treated wool specimens. The surface modification of the wool with the air plasma assisted the wool in obtaining darker color, better fixation, and uniform dyeing.

3.7. Tensile strength and tear strength

The tensile energy was defined as the energy required to extend the substance. This demonstrated the ability of a substrate to withstand external stress during extension. The textile materials had a physical and chemical nature to the fiber, the weave type, and the yarn twist, which were responsible for the frictional forces between the fibers and the yarns. The etching effect of the plasma on the textile fibers could alter these properties, as it is a surface phenomenon that could improve frictional forces. The tensile force and the tear strength of wool specimens were measured after the DBD plasma treatment (figure 9). The plasma treatment significantly improved the tensile strength of the wool specimens in both the warp and the weft directions, due to an increased amount of contact points and the breaking of chemical bonds in the outermost layer of the wool fiber [38, 39]. The treated wool specimens obtained a loss of tear strength in regard to the treatment time. Despite an increased number of contact points between the fibers and the yarns, the tear slit easily propagated, because of a higher cohesive force between the fibers and the yarns. This led to the breaking of fibers and yarns on the application of force, rather than the sliding action [1, 6, 40]. The samples exhibited a lower tear strength after plasma treatment.

4. Conclusions

The DBD plasma were used to enhance the physicochemical properties of wool fibers. The surface properties were largely dependent on treatment durations. The DBD treated wool specimens obtained improved wettability, wick ability, surface energy, and mechanical strength. The XPS results confirmed that the C–C/C–H content decreased and the C=O, C–O, C–N contents increased in correlation to the treatment time. The FTIR spectra also confirmed that the treatment decreased the amount of CH_2 and the CH_3 groups due to the oxidative splitting of the fatty layer. The cystic acid from breakage of disulfide linkages (–S–S–) in the hydrophobic layer of the wool increased. The treatment also damaged to the hydrophobic fatty acid layer in the scale structure of the wool fiber. Thus new pores and channels were generated. As a result of these improvements, the surface energy, the water droplet contact angles, and the wicking heights were significantly improved. The treatment also improved the coloration properties of the fiber, including the high color strength at low dye concentration, the better exhaustion of dye molecules, the good fixation, and the color uniformity of Reactive Red 195 on the wool substrate. The fastness properties of the plasma treated specimens obtained a grading of 4–5 for wash and light fastness, and 3–4 for rubbing fastness. The tensile strength of the treated specimens increased significantly. Their tear strength decreased slightly, due to the increased contact points following the plasma treatment.

Acknowledgments

This work was financially supported by the China National Textile & Apparel Council (2013'Textile Vision' Applied Basic Research, 2013-153) and the Collaborative Innovation Plan of Hubei Province for Key Technology of Eco-Ramie Industry (2014–8).

References

[1] Shahidi S, Ghoranneviss M and Sharifi S D 2014 *J. Fusion Energy* **33** 177
[2] Oliveira F R *et al* 2013 *J. Appl. Polym. Sci.* **128** 2638
[3] Molakarimi M, Khajeh Mehrizi M and Haji A 2016 *J. Textile Inst.* **107** 1314
[4] Haji A, Qavamnia S S and Bizhaem F K 2016 *Ind. Textila* **67** 244
[5] Ceria A *et al* 2010 *J. Mater. Process. Technol.* **210** 720
[6] Kan C W, Yuen C W M and Hung O N 2013 *Surf. Coat. Technol.* **228** S588
[7] Haji A and Qavamnia S S 2015 *Fibers Polym.* **16** 46
[8] Kan C-W *et al* 2014 *Carbohydr. Polym.* **102** 167
[9] Oliveira F R, Zille A and Souto A P 2014 *Appl. Surf. Sci.* **293** 177
[10] Kan C 2006 *Fibers Polym.* **7** 262
[11] Wang X *et al* 2015 *Appl. Surf. Sci.* **342** 101
[12] Canbolat S, Kilinc M and Kut D 2015 *Proc. Soc. Behav. Sci.* **195** 2143
[13] Chen C *et al* 2016 *Fibers Polym.* **17** 1181
[14] Kan C W, Chan K and Yuen C W M 2004 *Autex Res. J.* **4** 37
[15] Cui N-Y and Brown N M D 2002 *Appl. Surf. Sci.* **189** 31
[16] Zhong Y and Netravali A N 2016 *Surf. Innov.* **4** 3
[17] Bußler S *et al* 2015 *J. Food Eng.* **167** 166

[18] El-Zawahry M M, Ibrahim N A and Eid M A 2006 *Polym-Plast. Technol.* **45** 1123
[19] Eren E *et al* 2015 *J. Electrost.* **77** 69
[20] Ayati Najafabadi S A A *et al* 2012 *Surf. Eng.* **28** 710
[21] Helmke A *et al* 2009 *New J. Phys.* **11** 115025
[22] Bhatt S, Pulpytel J and Arefi-Khonsari F 2015 *Surf. Innov.* **3** 63
[23] Oliveira M S *et al* 2010 *Surf. Eng.* **26** 519
[24] Liu C *et al* 2004 *Surf. Coat. Technol.* **185** 311
[25] Kan C W and Yuen C W M 2006 *J. Mater. Process. Technol.* **178** 52
[26] Kusano Y *et al* 2017 *Surf. Eng.* 1
[27] Zanini S *et al* 2017 *Appl. Surf. Sci.* **427** 90
[28] Zhang R and Wang A 2015 *J. Clean. Prod.* **87** 961
[29] Haji A, Mehrizi M K and Sharifzadeh J 2016 *Fibers Polym.* **17** 1480
[30] Gupta M C and Pandey R R 1988 *J. Polym. Sci., Part A: Polym. Chem.* **26** 491
[31] Kikani P *et al* 2013 *Surf. Eng.* **29** 211
[32] Wang C X *et al* 2015 *Appl. Surf. Sci.* **349** 333
[33] Wang C X and Qiu Y P 2007 *Surf. Coat. Technol.* **201** 6273
[34] Liu C *et al* 2000 *Surf. Eng.* **16** 215
[35] Sajed T *et al* 2018 *Int. J. Biol. Macromol.* **107** 642
[36] Atav R and Yurdakul A 2011 *Fibres Text. East. Eur.* **85** 84
[37] Barani H and Haji A 2015 *J. Mol. Struct.* **1079** 35
[38] Naebe M *et al* 2010 *Text. Res. J.* **80** 312
[39] Naebe M *et al* 2013 *J. Text. Inst.* **104** 600
[40] Cheng S *et al* 2010 *Vacuum* **84** 1466